Reactivity of the 4d Transition Metals toward N Hydrogenation and NH Dissociation: A DFT-Based HSAB Analysis

Paul Crawford and P. Hu*

School of Chemistry, The Queen's University of Belfast, Belfast, BT9 5AG, U.K.

Received: September 2, 2005

The density functional theory (DFT) based hard−soft acid−base (HSAB) reactivity indices, including the electrophilicity index, have been successfully applied to many areas of molecular chemistry. In this work we test the applicability of such an approach to fundamental surface chemistry. We have considered, as prototypical surface reactions, both the hydrogenation of atomic nitrogen and the dissociative adsorption of the NH molecular radical. By use of a DFT methodology, the minimum energy reaction pathways, and corresponding reaction barriers, of the above reactions over Zr(001), Nb(110), Mo(110), Tc(001), Ru(001), Rh(111), and Pd(111) have been determined. By consideration of the chemical potential and chemical hardness of the surface metal atoms, and the principle of electronegativity equalization, it is found that the charge transferred to the NH radical during the process of dissociative adsorption correlates very well with that determined by Mulliken population analysis. Furthermore, it is found that the stability of the NH/surface transition state complex relates directly to this charge transfer and that the trend in transition state stability predicted by a HSAB treatment correlates very strongly with that determined by DFT calculations. With regards to N hydrogenation, we find that during the course of the reaction, H loses cohesion to the surface, as it must migrate from a 3-fold hollow site to either a bridge or top site, to react with N. Partial density of states (PDOS) and Mulliken population analysis reveal that this loss of bonding is accompanied by charge transfer from H to the surface metal atoms. Moreover, by simple modeling, we show that the reaction barriers are directly proportional to this mandatory charge transfer. Indeed, it is found that the reaction barriers correlate very well with the electrophilicity index of the metal atoms.

1. Introduction

The first steps toward revealing that the conceptual hard−soft acid−base (HSAB) theory[1−3] had a theoretical foundation in density functional theory were taken by Parr et al.[4] They showed that the Lagrangian multiplier (μ) in the Euler equation could be written as the partial derivative of the system's energy with respect to electron number at constant external potential

$$\mu = \left(\frac{\partial E}{\partial N}\right)_v \tag{1}$$

μ is commonly called the chemical potential and is characteristic of the system of interest. Furthermore, by relating eq 1 to Iczkowski and Margrave's definition of electronegativity[5]

$$\chi = -\left(\frac{\partial E}{\partial N}\right)_Z \tag{2}$$

a system's electronegativity and chemical potential were shown to be analogous.

In later work Parr and Pearson defined chemical hardness (η) as the second derivative of the system's ground-state energy with respect to electron number at constant external potential[6]

$$2\eta = \left(\frac{\partial^2 E}{\partial N^2}\right)_v = \left(\frac{\partial \mu}{\partial N}\right)_v \tag{3}$$

It is commonplace to use finite difference approximations to both μ and η, which are obtained using the ionization energy and electron affinity of the respective species

$$\mu = -\frac{1}{2}(I + A) \qquad \eta = \frac{1}{2}(I - A) \tag{4}$$

We can see that the finite difference approximation to μ is that of Mulliken's definition of electronegativity.[7]

Moreover, by considering Sanderson's principle of electronegativity equalization,[8,9] the following two equations were derived which are basic statements of the HSAB theory[6,10]

$$\Delta N = \frac{\mu_A - \mu_B}{2(\eta_A + \eta_B)} \tag{5}$$

$$\Delta E = -\frac{(\mu_A - \mu_B)^2}{4(\eta_A + \eta_B)} \tag{6}$$

Equation 5 gives a first approximation to the fractional number of electrons transferred (ΔN) as two systems, A and B, come together to react. The associated energy change is given by eq 6.

Of course this is only a part of the total energy change, which must include covalent bonding and ionic interactions. Nevertheless, eqs 5 and 6 are still very useful as chemical reactivity indices, as they measure the initial interaction between species A and B, using properties of the isolated systems. Moreover, as pointed out by Pearson,[11] values predicted by eqs 5 and 6 should show some proportionality to covalent bond strength,

* Corresponding author: p.hu@qub.ac.uk.

10.1021/jp054979s CCC: $33.50
Published on Web 02/08/2006

where coordinate bonding is involved. For neutral species, the degree of ionic bonding is also dependent on ΔN.

Equation 5 has proven useful in predicting both trends in reaction rate and bonding energies. In the oxidative addition of iron, by a series of X−Y molecules (X = I, CN, Cl and Y = H, CH_3), the reaction rate was found to correlate with ΔN as calculated by eq 5.[12] With regards to bond strength, the binding of CO to neutral transition metals was found to correlate with ΔN.[13] Namely, the trend in ΔN values was found to agree well with that of the mean bond strength of the metal carbonyls.

In a further development Maynard et al. found the ratio of electronegativity (Mulliken) squared to hardness to correlate well with reaction rate.[14] In a fluorescence decay study of the interaction of a series of electrophilic ligands with the NCp7 protein of HIV, the above ratio calculated for the various ligands was found to correlate well with the measured rate of reaction.[14] This work led Parr et al. to the concept of maximal electron flow and the derivation of the electrophilicity index[15]

$$\omega = \frac{\mu^2}{2\eta} \tag{7}$$

The electrophilicity index has since been successfully correlated with both trends in bonding energy and reaction rate for molecular species. Olah et al. found good agreement between the electrophilicity indices of a series of silylenes and germylenes and their complexation energy with NH_3.[16] Campodonico et al. found correlation between the electrophilicity indices of a series of thiocarbonates and their reaction rates with piperidine.[17]

It is evident that the DFT based HSAB reactivity indices have proven useful in helping to explain aspects of molecular reactivity. However, to the best of our knowledge these ideas have yet to be applied directly to surface chemistry and catalysis. Of particular importance is the surface chemistry of the transition metals due to their place in catalysis. Indeed some of the most important reactions to modern society occur over transition metal surfaces, e.g., the industrial production of ammonia,[18−27] the oxidation of CO to CO_2,[28−38] and hydrocarbon production by the Fischer−Tropsch reactions.[39−45] There is therefore an ever increasing need to understand the reactivity of transition metal surfaces toward these important reactions in order that the efficiency and specificity of current systems may be improved.

Simply speaking, surface reactions may be categorized as either an association reaction (bond forming) or dissociative (bond breaking). The former may occur by either a Langmuir−Hinshelwood (L−H) mechanism, where both reactants are preadsorbed, or an Eley-Rideal (E−R) mechanism, where one reactant is preadsorbed and the second reactant is in the gas phase. In this DFT study, we analyze the reactivity of both N hydrogenation, occurring by the L−H mechanism (a bond-forming process), and the dissociative adsorption of NH (a bond breaking process) on the surfaces of the 4d transition metals using the DFT-based HSAB reactivity indices. The hydrogenation of N is of particular importance as it is the first hydrogenation step in ammonia synthesis. These processes were modeled on Zr(001), Nb(110), Mo(110), Tc(001), Ru(001), Rh(111), and Pd(111). The most stable adsorption sites for reactants and the most stable transition state geometries have been identified. The reaction barriers discussed in this work correspond to the lowest energy reaction pathways.

2. Calculation Method

Our DFT calculations were performed using the CASTEP code.[46] The effects of electron exchange and correlation were approximated by the generalized gradient approximation (GGA) functional of Perdew, Burke and Ernzerhof (PBE).[47] Ultrasoft pseudopotentials were used to describe the ionic cores, and the valence states were expanded in a plane wave basis set up to 360 eV cutoff energy. The surfaces were modeled by four layers of metal atoms repeated periodically within a p(2 × 2) unit cell. The top layer was relaxed, while the three lower layers were fixed at their bulk truncated positions. The 3 × 3 × 1 *k*-point sampling was found to be adequate for the unit cells used in this study. In all the calculations the vacuum region between the slabs was over 10 Å. The transition states were located by the constrained minimization technique, which constrains the distance between the reacting atoms while optimizing the remaining degrees of freedom. Transition states were identified when (i) the forces on the atoms were zero and (ii) the energy was a maximum along the reaction coordinate, but a minimum with respect to all the remaining degrees of freedom. Further calculation details can be obtained from ref 48.

TABLE 1: ΔE_{diss} Is a Measure of Transition State Stability As Given by Eq 8, Σq^{TS} Is the Total Mulliken Charge on the NH Molecule at the Transition State, and η and μ Are the Finite Difference Approximations to the Metal Hardness and Chemical Potential, Respectively

surface	ΔE_{diss} (eV)	Σq^{TS} (electrons)	η (eV)	μ (eV)
Zr(001)	−5.78	−0.89	3.10	−3.53
Nb(110)	−4.56	−0.80	2.93	−3.83
Mo(110)	−4.65	−0.71	3.17	−3.92
Tc(001)	−4.12	−0.58	3.36	−3.91
Ru(001)	−3.59	−0.55	3.16	−4.21
Rh(111)	−3.34	−0.47	3.16	−4.30
Pd(111)	−2.85	−0.28	3.89	−4.45

3. Results and Discussion

3.1. The Dissociative Adsorption of NH. We will first consider the process of dissociation on transition metal surfaces and whether the HSAB principles are useful in explaining the variation in reactivity from one surface to the next. As a simple model system we have considered the dissociative adsorption of the NH molecular radical; this is mainly in the interest of consistency and convenience as the formation of NH is considered in the next section. Our calculations show that at the transition state, the NH axis is parallel to the surface with N at a hollow site and H at either a bridge site or hollow site depending on the metal surface. The stability of the transition state is given by[49,50]

$$\Delta E_{diss} = E^{TS}(\text{NH/surface}) - \{E(\text{surface}) + E(\text{NH})_{gas}\} \tag{8}$$

where E^{TS}(NH/surface), E(surface), and $E(NH)_{gas}$ are the total energies of the transition state complex, the clean surface, and the NH molecule in the gas phase, respectively. The calculated values are given in Table 1. For this dissociation process, reactivity is completely determined by the stability of the molecule/surface transition state complex, as the initial state is always a clean surface and the gas-phase molecule.

Our calculated chemical potential and hardness for the NH molecule are −7.047 and 6.586 eV, respectively. The chemical potential of NH is seen to be greater than any of the 4d transition metals considered in this study (Table 1). Thus, if we consider the Blyholder model[51] as a description of the interaction of NH with the surface metal atoms, then clearly electron donation from the metal to the molecule will predominate due to the larger chemical potential of NH. It has been pointed out by Pearson[11] that in cases where ΔN is moderate and predominantly in one

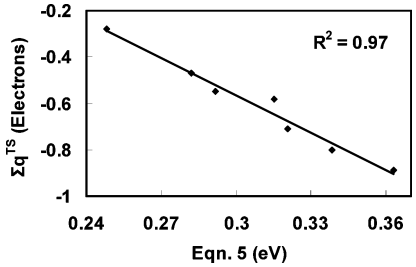

Figure 1. The total Mulliken charge on the molecule at the transition state (Σq^{TS}), plotted against the charge predicted by eq 5.

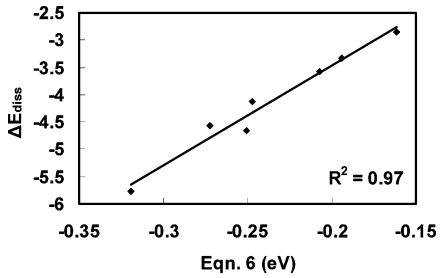

Figure 2. Transition state stability (ΔE_{diss}) plotted against values predicted by eq 6.

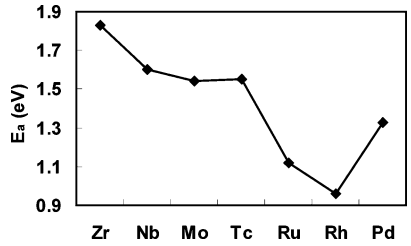

Figure 3. Our calculated reaction barriers for N + H → NH over the 4d transition metals from Zr−Pd.

direction and that orbital interactions can be considered constant, e.g., the interaction of a series of similar metals with a ligand, then eqs 5 and 6 should be useful.

To test the validity of eq 5 for this system, we have calculated the total charge (Σq^{TS}) on the NH molecule at the transition state on the various metals via Mulliken population analysis (Table 1). The values from our Mulliken population analysis are plotted against those values predicted by eq 5 in Figure 1. As can be seen the correlation is very good with $R^2 = 0.97$.

To test whether the actual stability of the transition state on the surface is related to this observed charge transfer, we have plotted our calculated DFT energy values (Table 1) against those predicted by eq 6 (Figure 2). Here again the correlation is observed to be very good, indicating that the stability of the transition state complexes on the surfaces is indeed related to the charge-transfer processes from the surface atoms to the molecule.

3.2. The Hydrogenation of Atomic Nitrogen. We now consider the process of bond formation by analyzing the reactivity of N + H → NH over the selected metals. As most association reactions occur by the L−H mechanism, the E−R mechanism is not considered in this work. Our calculated reaction barriers for N + H are plotted in Figure 3. The values are also given in Table 2. The curve is observed to have an interesting stepped nature, where Ru(001) and Rh(111) are seen to be the best hydrogenation catalysts. This is consistent with the fact that Ru is known to be a good ammonia synthesis catalyst.

The reaction barriers for N + H → NH depend not only on the stability of the transition state but also on the stability of N and H on the surface in the initial state. An important question is then, how does the stability of N and H on the surface change on moving along reaction coordinate from the initial state to the transition state? We have found that during transition state formation N moves very little from its initial state position, and its bonding to the surface is only slightly weakened. H on the other hand is observed to migrate from a hollow site to either a top site or bridge site during the course of the reaction. This situation is always going to result in significant loss of bonding between H and the surface.

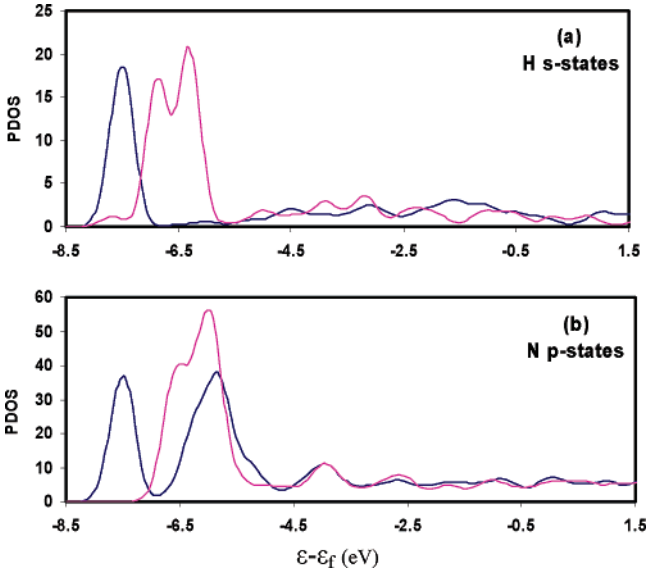

Figure 4. (a) Density of states projected onto s states of H at the transition state (blue line) and initial state (pink line). (b) Density of states projected onto p states of N at transition state (blue line) and initial state (pink line). PDOS are in arbitrary units.

TABLE 2: E_a Is the Activation Energy for N + H → NH over the 4d Metals from Zr to Pd, Δq Is the Charge (electrons) Transferred to the Surface Metal Atoms during the Course of the Reaction As Determined by Mulliken Charge Analysis, and ω Is the Electrophilicity Index of the Various Metals Calculated Using Atomic Parameters

surface	E_a (eV)	Δq	ω (eV)
Zr(001)	1.83	0.29	2.00
Nb(110)	1.60	0.27	2.50
Mo(110)	1.54	0.23	2.42
Tc(001)	1.55	0.25	2.28
Ru(001)	1.12	0.23	2.80
Rh(111)	0.96	0.22	2.92
Pd(111)	1.33	0.15	2.54

To analyze further the changes in reactants in going from the initial state to the transition state, we calculated the Mulliken charge on N and H in the initial state and compared these values to their respective charges at the transition state. This analysis, although only qualitative, reveals a net loss of charge during transition state formation (Table 2). This loss of charge is mainly associated with the decrease in bonding strength of hydrogen in moving from a hollow site to a site of lower coordination during the course of the reaction.

More is revealed about the observed charge transfer and the associated changes in bonding during the course of the reaction by a partial density of states analysis. In Figure 4a, the density of states is projected onto the s states of H at both the initial state (pink line) and transition state (blue line); in Figure 4b, the density of states is projected onto the p states of N, again at the initial state (pink line) and transition state (blue line). Considering Figure 4b first, we can see that in going from

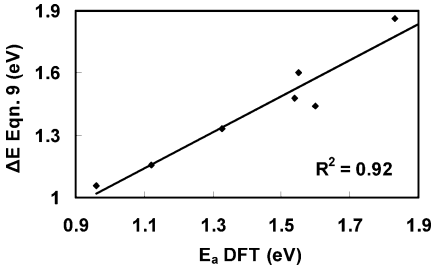

Figure 5. Correlation between ΔE calculated by eq 9 when $\Delta N \sim 1.1$ and $c \sim 3.9$ and DFT reaction barriers.

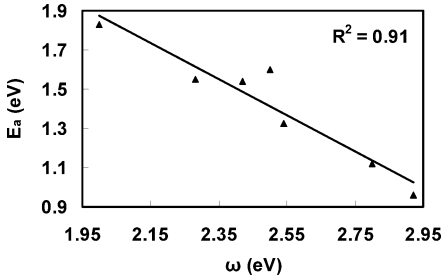

Figure 6. Correlation between reaction barriers (E_a) for N + H → NH over the 4d transition metals calculated by DFT and metal electrophilicity index (eq 7).

the initial state to the transition state the main peak at around −6.5 eV decreases in area and a second peak appears around −7.5 eV. Examination of the quantum states at around −7.5 eV revels that the appearance of the second peak is associated with the onset of bonding between N and H at the transition state. It should be noted that the area of the N−H bonding peak is approximately equal to the area lost in the initial state peak. This would imply that electron density is donated from N into the newly formed N−H bonding orbital and not transferred to the surface metal atoms. Examining now Figure 4a, we can see that a peak also appears at around −7.5 eV in going from the initial state to transition state confirming the onset of N−H bonding. However, both initial state peaks, at around −6 and −7 eV, disappear; this indicates a net loss in electron density on hydrogen in going from the initial state to the transition state; i.e., charge is transferred to the surface metal atoms.

It is therefore evident that during transition state formation H must lose some degree of bonding to the surface in order to form a bond with N, which is reasonable considering the valency of H is 1. This loss of bonding is observed to be associated with charge depletion on H. Therefore electron density must be lost to the surface in order for the transition state to form. Since we are considering the same reaction occurring over a series of similar metals (from the same period), one could envisage that the changes in orbital interactions during the course of the reactions could be considered almost constant across the transition series. Furthermore, if other effects are considered constant or negligible, this mandatory electron transfer may be responsible for the observed trend in the reaction barriers. To test this hypothesis we can approximate the energy change associated with this charge depletion and see if it correlates with the calculated trend in reaction barrier.

If we consider that the charge transfer to the surface is almost constant across the series, which is a reasonable assumption since we are considering the same elementary reaction step, then the energy change associated with this process may be modeled by a standard electron-transfer equation[10,15]

$$\Delta E = \Delta N \mu_M + \Delta N^2 \frac{1}{2} \eta_M + c \qquad (9)$$

where μ_M and η_M are the chemical potential and hardness of the various metals, respectively. When $\Delta N \sim 1.1$ and $c \sim 3.9$, ΔE predicted by eq 9 correlates very well with our DFT reaction barriers (Figure 5).

The above results suggest that this charge transfer from H to the surface metal atoms during transition state formation is indeed responsible for the observed trend in reactivity. Moreover, by considering the fact that electrophilicity describes the propensity of a species to accept electrons and that this concept has now been quantified in terms of the electrophilicity index,[14,15] one would expect some agreement between the electrophilicity indices of the metal atoms and the reaction barriers. This is exactly what we find; a good correlation between our calculated DFT barriers and the electrophilicity index of the metals (eq 7) is seen to exist (Figure 6).

Thus, the more electrophilic the metal, the lower the reaction barrier. Namely, under the assumption that this reaction occurs by a mandatory charge transfer to the surface and that the amount of charge is almost constant across the 4d series, then the more electrophilic the metal, the more energetically favorable it is for the electron transfer to occur and thus the lower the resulting reaction barrier. It should be noted that in all of the above calculations atomic ionization energies and electron affinities were used in the approximations of μ and η. The fact that atomic ionization energy and electron affinity are applicable here is not entirely surprising as evidence exists showing chemisorption to be a very local phenomenon. Tight binding calculations by Zheng, Apeloig, and Hoffmann[52] have shown that top-site adsorption of CH_3 on Co(001) involves charge being transferred mainly from the Co atom involved directly in the bonding. In addition, a detailed DFT study on the interaction of CO and O with Pt(111) by Bleakley and Hu[53] has provided further insight into the local nature of chemisorption. By examination of two-dimensional contour plots of the total valence charge density, it was found that the chemisorbed O atom or CO molecule does not significantly affect the charge distribution of next neighbor Pt atoms.

4. Conclusion

In this work we have used the HSAB reactivity descriptors in an analysis of chemical reactivity on surfaces. We have shown that the stability of the N−H transition state complex on the surface is inherently related to a charge transfer process from the surface metal atoms to the molecule. Thus, the activation energy for the dissociative adsorption of NH is directly related to the energy change associated with this charge transfer.

We have given a detailed analysis of how electron distribution changes as N and H react on the metal surfaces. We have found that as the reaction proceeds electron density is lost mainly from hydrogen to the surface metal atoms; charge on N is observed to be almost constant. We have also found a good correlation between the electrophilicity index of the metal and the corresponding reaction barrier. Thus, for N + H → NH over the 4d metals the trend in reactivity is related to how energetically favorable it is to transfer electron density to the surface atoms during the course of the reaction.

References and Notes

(1) Pearson, R. G. *J. Am. Chem. Soc.* **1963**, *85*, 3533.
(2) Pearson, R. G. *Hard and Soft Acids and Bases*; Dowden, Hutchison and Ross: Stroudsburg, PA, 1973.
(3) Pearson, R. G. *J. Chem. Educ.* **1968**, *45*, 581.
(4) Parr, R. G.; Donnelly, R. A.; Levy, M.; Palke, W. E. *J. Chem. Phys.* **1978**, *68*, 3801.

(5) Iczkowski, R. P.; Margrave, J. L. *J. Am. Chem. Soc.* **1961**, *83*, 3547.
(6) Parr, R. G.; Pearson, R. G. *J. Am. Chem. Soc.* **1983**, *105*, 7512.
(7) Mulliken, R. S. *J. Chem. Phys.* **1934**, *2*, 782.
(8) Sanderson, R. T. *Science* **1951**, *114*, 670.
(9) Sanderson, R. T. *Chemical Bonds and Bond Energy*, 2nd ed.; Academic Press: New York, 1976.
(10) Parr, R. G.; Yang, W. *Density Functional Theory of Atoms and Molecules*; Oxford University Press: Oxford, 1989.
(11) Pearson, R. G. *Coord. Chem. Rev.* **1990**, *100*, 403.
(12) Pearson, R. G. *Inorg. Chem.* **1988**, *27*, 734.
(13) Pearson, R. G. *Inorg. Chem.* **1984**, *23*, 4675.
(14) Maynard, A. T.; Huang, M.; Rice, W. G.; Covell, D. G. *Proc. Natl. Acad. Sci. U.S.A.* **1998**, *95*, 11578.
(15) Parr, G.; Szentpaly, L. V.; Liu, S. *J. Am. Chem. Soc.* **1999**, *121*, 1922.
(16) Olah, J.; De Proft, F.; Veszpremi, T.; Greelings, P. *J. Phys. Chem. A* **2005**, *109*, 1608.
(17) Campodonico, P. R.; Fuentealba, P.; Castro, E. A.; Santos, J. G.; Contreras, R. *J. Org. Chem.* **2005**, *70*, 1754.
(18) Aika, K. I.; Tamaru, K. in *Ammonia: Catalysis and Manufacture*; Nielson, A., Ed.; Springer-Verlag: Berlin, 1995.
(19) Ertle, G. *Catal. Rev.-Sci. Eng.* **1980**, *21*, 201.
(20) Tennison, S. R. In *Catalytic Ammonia Synthesis Fundamentals and Practice*; Jennings, J. R., Ed.; Plenum: New York, 1991.
(21) Somorjai, G. A. *Introduction to Surface Chemistry and Catalysis*; Wiley: New York, 1994.
(22) Hagen, S.; Barfod, R.; Fehrmann, R.; Jacobsen, C. J. H.; Teunissen, H. T.; Chorkendoff, Ib. *J. Catal.* **2003**, *214*, 327.
(23) Logadottir, A.; Norskov, J. K. *J. Catal.* **2003**, *220*, 273.
(24) Siporin, S. E.; Davis, R. J.; Rarog-Pilecka, W.; Szmigiel, D.; Kowalczyk, Z. *Catal. Lett.* **2004**, *93*, 61.
(25) Hinrichsen, O.; Rosowski, F.; Hornung, A.; Muhler, M.; Ertle, G. *J. Catal.* **1997**, *165*, 33.
(26) Dietrich, H.; Jacobi, K.; Ertle, G. *J. Chem. Phys.* **1997**, *106*, 9313.
(27) Dahl, S.; Taylor, P. A.; Tornqvist, E.; Chorkendorff, I. *J. Catal.* **1998**, *178*, 679.
(28) Ertle, G. *Surf. Sci.* **1994**, *299*, 742.
(29) Stampfl, C.; Scheffler, M. *Phys. Rev. Lett.* **1997**, *78*, 1500.
(30) Yeo, Y. Y.; King, D. A. *J. Chem. Phys.* **1997**, *106*, 392.
(31) Alavi, A.; Hu, P.; Deutsch, T.; Silvestrelli, P. L.; Hutter, J. *Phys. Rev. Lett.* **1998**, *80*, 3650.
(32) Bottcher, A.; Conrad, H.; Niehus, H. *Surf. Sci.* **2000**, *452*, 125.
(33) Wang, J.; Fan, C. Y.; Jacobi, K.; Ertle, G. *Surf. Sci.* **2001**, *481*, 113.
(34) Fan, C. Y.; Wang, J.; Jacobi, K.; Ertle, G. *J. Chem. Phys.* **2001**, *114*, 10058.
(35) Bottcher, A.; Niehus, H.; Schwegmann, S.; Over, H.; Ertle, G. *J. Phys. Chem. B* **1997**, *101*, 11185.
(36) Over, H.; Kim, Y. D.; Seitsonen, A. P.; Wendt, S.; Lundgren, E.; Schmid, M.; Varga, P.; Morgante, A.; Ertle, G. *Science* **2000**, *287*, 1474.
(37) Hendriksen, B. L. M.; Frenken, J. W. M. *Phys. Rev. Lett.* **2002**, *89*, 046101.
(38) Daniell, W.; Weingand, T.; Knozinger, H. *J. Mol. Catal. A*: *Chem.* **2003**, *204*, 519.
(39) Gong, X.-Q.; Ravel, R.; Hu, P. *J. Chem. Phys.* **2005**, *122*, 024711.
(40) Vannice, M. A. *Catal. Rev.−Sci. Eng.* **1976**, *14*, 153.
(41) Schulz, H. *Appl. Catal., A* **1999**, *186*, 3.
(42) Schulz, H.; Claeys, M. *Appl. Catal., A* **1999**, *186*, 91.
(43) Dry, M. E. *Catal. Today* **2002**, *71*, 227.
(44) Davis, B. H. *Fuel Process. Technol.* **2001**, *71*, 157.
(45) Liu, Z.-P.; Hu, P. *J. Am. Chem. Soc.* **2002**, *124*, 11568.
(46) Payne, M. C.; Teter, M. P.; Allan, D. C.; Arias, T. A.; Joannopoulos, J. D. *Rev. Mod. Phys.* **1992**, *64*, 1045.
(47) Perdew, J. P.; Burke, K.; Ernzerhof, M. *Phys. Rev. Lett.* **1996**, *77*, 3865.
(48) Michaelides, A.; Hu, P. *J. Am. Chem. Soc.* **2000**, *122*, 9866.
(49) Hammer, B. *Phys. Rev. Lett.* **1999**, *83*, 3681.
(50) Dahl, S.; Tornqvist, E.; Chorkendorff, I. *J. Catal.* **2000**, *192*, 381.
(51) Blyholder, G. *J. Phys. Chem.* **1964**, *68*, 2772.
(52) Zheng, C.; Apeloig, Y.; Hoffmann, R. *J. Am. Chem. Soc.* **1988**, *110*, 749.
(53) Bleakley, K.; Hu, P. *J. Am. Chem. Soc.* **1999**, *121*, 7644.